

pPeOp from *Omphalia lapidescens* Schroet suppresses the proliferation of cervical cancer HeLa cells via JAK/STAT3 signaling pathway

Yan Chen, Zhenjie Fu, Yuqin Xu, Yitao Chen*, Peilei Pan*

School of Life Sciences, Zhejiang Chinese Medical University, Hangzhou 310053 China

*Corresponding authors, e-mail: cytworld@163.com, panplei@163.com

Received 19 Sep 2021, Accepted 5 May 2022

Available online 15 Jul 2022

ABSTRACT: pPeOp is a protein extracted from the sclerotium of *Omphalia lapidescens*. Several studies have shown its anti-carcinogenic effects. However, its functions in cervical cancer and the underlying cellular mechanisms are relatively unknown. Here, we examined the effect and molecular mechanism of pPeOp on HeLa cells. The MTS assay and EdU assay showed that pPeOp decreased HeLa cell viability and proliferation in a dose-dependent manner. Besides, the quantitative real-time PCR (qRT-PCR) and western blot analysis showed that the mRNA levels of JAK1, JAK2, GP130, and STAT3 and protein levels of STAT3 and p-STAT3 were significantly decreased, whereas the mRNA expression levels of SOCS1 and SOCS3 were significantly elevated in HeLa cells. Furthermore, Interleukin-6 (IL-6) and NSC74859 were used as the agonist and inhibitor of the JAK/STAT3 signaling pathway, respectively. The flow cytometry and MTS assay showed that the antitumor effect was increased when pPeOp was co-treated with IL-6, while decreased with inhibitor treatment. These results demonstrate that pPeOp could effectively inhibit the proliferation and viability of cervical cancer cells by regulating JAK/STAT3 signaling pathway, suggesting that pPeOp may serve as a novel therapeutic agent for cervical cancer.

KEYWORDS: cervical cancer, HeLa cells, JAK/STAT3, pPeOp, *Omphalia lapidescens*

INTRODUCTION

Cervical cancer was the fourth most common cancer in women [1, 2]. Although multimodal treatments, including surgery, radiotherapy, and chemotherapy, have improved, patients with cervical cancer still have poor prognosis [3, 4]. Therefore, it is of great importance to find an effective alternative to traditional treatment for cervical cancer with fewer side effects.

Omphalia lapidescens [5–7], one of the most important medical fungi in Traditional Chinese Medicine, was first recorded in Shennong Bencao Jing. It has the effect of softening hardness and transforming phlegm, used as deworming medicine frequently. However, recent studies have shown that it has significant antitumor properties. China Food and Drug Administration has approved *O. lapidescens* tablet and Leiwan capsule as antitumor auxiliary drugs [8]. pPeOp, a protein extracted from *Omphalia lapidescens* with PVP extraction buffer, has no toxicity to MC-1 normal gastric cells [9]. Previous studies demonstrated that pPeOp can negatively regulate the activity of JAK/STAT3 signaling pathway and significantly inhibits proliferation and induces apoptosis in gastric cancer cells and human colon cancer cells [8, 10–12]. To date, however, no studies have investigated its efficacy for treating cervical cancer.

Therefore, the present study aimed to investigate the inhibitory effect and mechanism of pPeOp in human cervical cancer cells. Our results confirmed that pPeOp has a markedly negative regulation effect on

JAK/STAT3 signaling pathway in HeLa cells and thus inhibits cell activity, proliferation, and cell cycle.

MATERIALS AND METHODS

Experimental materials and reagents

RPMI-1640 was provided from Genom Biomedical company (Hangzhou, China). TRIzol used in RNA extraction was provided from Thermo Fisher Scientific (Massachusetts, USA). Recombinant human IL-6 was purchased from Beyotime (Shanghai, China). NSC74859 was purchased from MedChemExpress (New Jersey, USA). Primers were purchased from Sangon Biological Technology (Shanghai, China). The primer sequences were listed in the Table 1. All antibodies were purchased from Cell Signaling Technology (Boston, USA).

pPeOp extraction and purification

The fruiting body of *Omphalia lapidescens* was purchased from Fang Hui Chun Tang (Hangzhou, China). pPeOp was a purified bioactive protein in *O. lapidescens* which was obtained using polyvinylpyrrolidone (PVP) followed by gel filtration chromatography. Protein extraction and purification were performed according to a previously published protocol [9].

Cell culture

Human cervical cancer cell lines, HeLa, obtained from the Zhejiang Provincial Center for Disease and Prevention Centre (Hangzhou, China) were cultured in RPMI-1640 supplemented with 10% fetal bovine serum

Table 1 Primer sequences for qRT-PCR.

Name	Primer F (sequence 5'-3')	Primer R (sequence 5'-3')
GAPDH	TGACTTCAACAGCGACACCCA	CACCCTGTTGCTGTAGCCAAA
GP130	TAGTGACCAGCAGTTATAT	CGACTACAGTGTCAAATAA
JAK1	CCTGCTGGTGGCTACTAAGA	AGATGTGTGTTCTCGTGCCT
JAK2	GCCTTCTTTTCAGAGCCATCA	CCAGGGCACCTATCCTCATA
STAT3	GACATGGAGTTGACCTCGGAGTG	GGTGGCAGAATGCAGGTAGGC
SOCS1	TCGCCCTTAGCGTGAAGA	CTGCCATCCAGGTGAAAGC
SOCS3	GCCACTCTTCAGCATCTCT	GGTCCAGGAACCTCCCGAAT

(Zhejiang Tianhang Biotechnology Co. Ltd., Huzhou, China) and 1% penicillin-streptomycin (Gibco, New York, USA) in a humidified atmosphere of 5% CO₂ at 37°C.

RNA extraction and quantitative real-time polymerase chain reaction (qRT-PCR)

TRIzol reagent was used to extract total RNA from cells. RNA reverse transcription was operated using Maxima First Strand cDNA Synthesis kit while real-time PCR was performed with the SYBR-Green Master Mix (Thermo Fisher Scientific, USA). qRT-PCR and data collection was conducted by means of Eppendorf Realplex 4 Real Time PCR Machine (Eppendorf, Saxony, Germany). The relative expression levels were evaluated by using the $2^{-\Delta\Delta Ct}$ method, and GAPDH served as an internal control.

Western blot analysis

HeLa cells were lysed with RIPA (Beyotime, China) supplemented with PMSF and the concentration of total protein was measured using BCA Protein Assay Kit (Solarbio, Beijing, China) according to the manufacturer's protocol. Equal amounts of protein were separated on a 10% SDS polyacrylamide gel and then transferred to a polyvinylidene difluoride (PVDF) membrane (Millipore, Massachusetts, USA). After being blocked with 5% skim milk for 2 h at room temperature, the membrane was incubated with primary antibodies (from CST, Boston, USA) against p-STAT3 (1:1000), STAT3 (1:1000) and GAPDH (1:1000) at 4°C overnight followed by a wash with TBST for 3 times. The membranes were incubated with HRP-conjugated goat anti-rabbit IgG (1:1000, Beyotime, China) at room temperature for 2 h and then washed in TBST for 3 times. The protein expression levels were detected by ECL STAR luminous solution (Beyotime, China) using Aplegen Gel Documentation System (OmegaLum G, San Francisco, USA). Protein gray values were analyzed by Image J software.

Cell cycle detected by flow cytometry

Cells in each group were first harvested with EDTA-free trypsin (0.25%), and cell density was adjusted to about 1×10^5 /ml. Then, the cells were fixed overnight with 1.0 ml 70% cold ethanol at 4°C. The cells were

washed with cold PBS and then incubated with 0.5 ml PI/RNase staining buffer (BD Biosciences, New Jersey, USA) for 15 min at room temperature in the dark. Cell cycle distribution was finally detected by a flow cytometer (Beckman FC500, Miami, USA).

MTS assay

Cell viability was determined using the MTS reagent (Promega, Wisconsin, USA) according to the manufacturer's instructions. At the same time, 20 μ l MTS was added to each well of 96-well plates, containing 100 μ l medium. After incubation for 4 h at 37°C in the dark, the absorbance at 490 nm of each well was measured using a microplate reader (BioTek Instruments, Vermont, USA).

EdU incorporation assay

The proliferation activity of cells was analyzed using the BeyoClick™ EdU Cell Proliferation Kit with Alexa Fluor 594 (Beyotime, China) according to the manufacturer's instructions. Briefly, cells were incubated with 10 μ M EdU in normal medium at 37°C for 2 h, followed by fixing with 4% formaldehyde for 30 min and permeating with 0.3% Triton X-100 for 10 min at room temperature. Then, the cells were incubated with 1 \times Apollo® reaction cocktail for 30 min at room temperature. Finally, the nuclear DNA was stained with Hoechst 33342 for 10 min. Samples were analyzed by a fluorescence microscope (ZEISS, Oberkochen Germany).

Statistical analysis

All experiments were repeated at least 3 times, the results were expressed as the mean \pm standard deviation (SD), and the statistical analysis was performed by SPSS 16.0 software (IBM Corp, Armonk, NY, USA) and GraphPad Prism 6 (GraphPad Software, Inc., San Diego, CA, USA). The comparison of 2 independent groups was detected by *t*-tests. One-way ANOVA was used for comparison among 3 or more groups. A *p*-value of < 0.05 was considered statistically significant.

RESULTS

Effects of pPeOp treatments in HeLa cells

Effect on morphology

Light microscopy was applied to analyze the morphological changes of the HeLa cells. When treated with PVP buffer (90 $\mu\text{g/ml}$), as shown in Fig. 1a, HeLa cells retained normal morphology compared to control cells. When exposed to 30–90 $\mu\text{g/ml}$ pPeOp, however, cells became markedly damaged, reverting to a spherical morphology and showing signs of shrinkage.

Effects on viability

HeLa cells were exposed to varying concentration of pPeOp or 90 $\mu\text{g/ml}$ PVP for 24 h, after which the cell viability was assayed by the MTS assay. As shown in Fig. 1b, when compared with control group, the inhibition of cell viability in HeLa cells became more significant with increasing concentration of pPeOp ($p < 0.05$). On the contrary, there was no significant difference in the viability of cells treated with PVP. These data indicated that pPeOp inhibited the viability of HeLa cells in a dose-dependent manner.

Effects on proliferation

The EdU assay was used to test cell proliferation ability. As shown in Fig. 1c, the relative EdU-positive cell numbers significantly decreased with increasing concentration of pPeOp ($p < 0.01$). In addition, there was no significant difference in the EdU-positive cell numbers with PVP. Our data demonstrated that the proliferation activity of HeLa cells was significantly inhibited by pPeOp.

Effects on JAK/STAT3 signaling pathways

STAT3, as a transcription factor, plays an important role in tumor cell proliferation and progression [13]. Therefore, we wondered if pPeOp could regulate the JAK/STAT3 pathway in HeLa cells. Results showed that the mRNA levels of JAK1, JAK2, GP130, and STAT3 and protein levels of STAT3 and p-STAT3 were significantly decreased, whereas the mRNA expression levels of SOCS1 and SOCS3 were significantly elevated in HeLa cells (Fig. 2).

Screening for optimum concentration of agonists and inhibitors

MTS and RT-qPCR were used to determine the optimal concentration of agonists and inhibitors for further experiment. As shown in Fig. 3a-d, in cervical cancer HeLa cells, the mRNA expression level of STAT3 and cell viability were significantly elevated after being treated with 100 ng/ml IL-6, and the opposite was treated with 50 ng/ml NSC74859. Thus, the most optimum concentration of IL-6 and NSC74859 is 100 ng/ml and 50 ng/ml, respectively.

Effects of IL-6 and NSC74859 on pPeOp regulation of cell viability and cell cycle

In order to further study the role of JAK/STAT3 signal pathway in the anticancer of pPeOp, we studied the cell viability of cervical cancer cells when the agonist and inhibitor of the JAK/STAT3 signaling pathway and pPeOp acted together or alone. The MTS assay results (Fig. 3e) showed that cell proliferation was slowed in the treatment with pPeOp alone group compared with that in the control group. pPeOp in the combination with IL-6 and NSC74859 could inhibit 57.11% and 23.61% of cells, respectively. These data indicated that pPeOp significantly inhibited the activity of HeLa cells, and IL-6 significantly enhanced the inhibitory effect of pPeOp on the activity, whereas NSC74859 weakened the effect. To further investigate the mechanism of pPeOp-induced suppression of HeLa cell proliferation, the cell cycle distribution of HeLa cells was determined by flow cytometry. Our results (Fig. 3f,g) showed that pPeOp induced HeLa cell cycle arrest in S phase. The blocking of pPeOp was enhanced by IL-6, while weakened with NSC74859.

DISCUSSION

Despite cervical cancer being now preventable in the developed world, it is still the leading cause of death in developing nations with limited access to care. At present, most of chemical drugs and radiotherapy methods for cervical cancer treatment have serious side effects [14, 15]. Previous studies have shown that *O. lapidescens* can effectively inhibit tumor growth, and its negative regulation of JAK/STAT3 signaling pathway is one of the main mechanisms for its anticancer effect [8].

The JAK/STAT signaling pathway is mainly composed of 2 genes, JAK and STAT, which jointly participate in the response of various cytokines and growth factors, including cell proliferation, differentiation, migration, apoptosis, and cell survival, through the transfer of extracellular information to the nucleus [16, 17]. JAKs are a class of non-receptor tyrosine kinases, which generally need to bind to receptors to form complete receptor/kinase signal transduction functions [18]. The STAT family consists of 7 members: STAT1, STAT2, STAT3, STAT4, STAT5A, STAT5B, and STAT6 [19, 20]. Each STAT has 7 conservative characteristics: NH2 terminal domains (ND), Coiled-coil, DNA-binding domains (DBD), Linker, and Src homology 2 domain (SH2), followed by a transcriptional activation domains (TAD) at the C-terminal [21]. STATs are both a signal transducer and a transcription factor. After activation by tyrosine phosphorylation, STATs dimerized and transferred to the nucleus, where they play an active transcription role by binding to corresponding sites on promoters [13]. Previous studies have shown that abnormal activation of JAK/STAT3 signaling pathway has been found in many diseases, es-

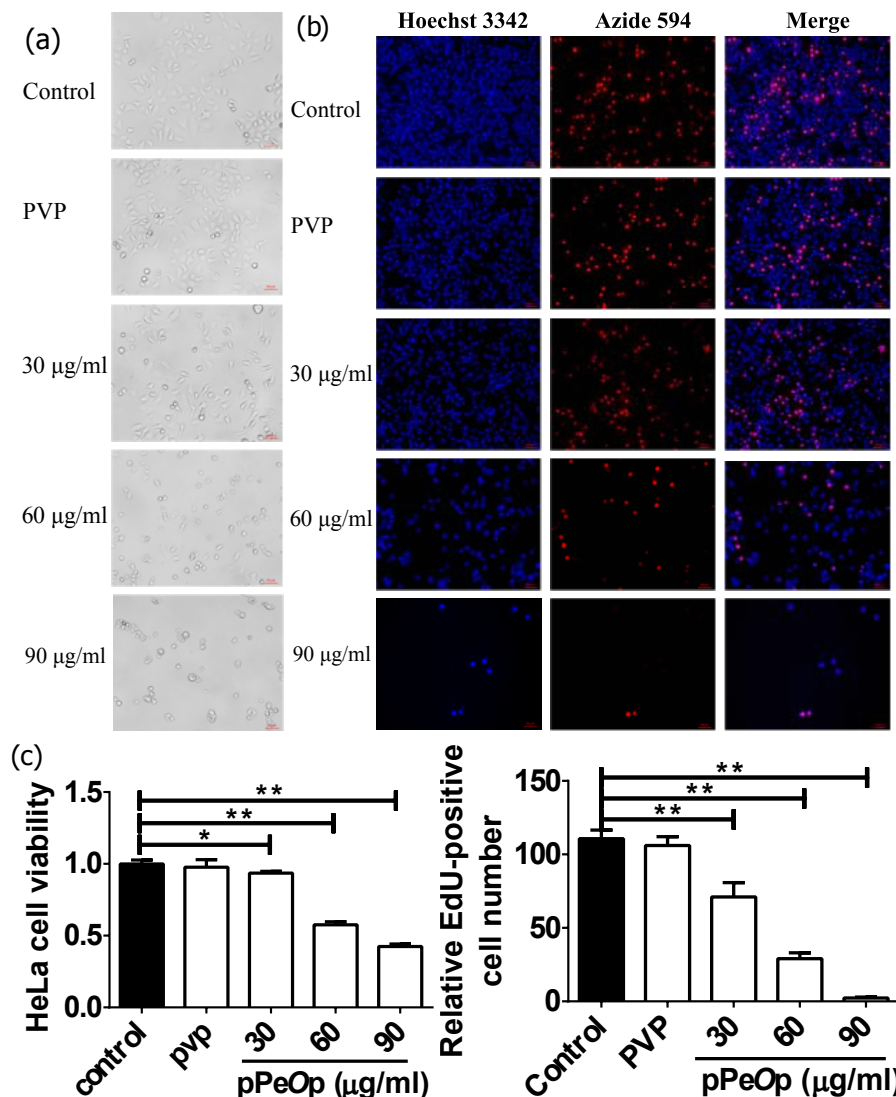


Fig. 1 Treatment effects of pPeOp on HeLa cells. Cells were treated with PVP (90 µg/ml) or pPeOp (30, 60, and 90 µg/ml) for 24 h. (a) Cell morphology observed by light microscope. (b) Cell viability detected by MTS assay. (c) Cell proliferation activity tested by EdU assay. EdU-positive cells were counted under the fluorescence microscope after 2 h. * $p < 0.05$ and ** $p < 0.01$ vs. control group.

pecially breast cancer [22], lung cancer [23], liver cancer [24], ovarian cancer [25], and other tumors [13].

STAT3 is currently recognized as a very promising target for cancer therapy. Although current studies are not enough to reach the stage of clinical application, STAT3 has long been identified as a typical oncogene [26, 27]. The JAK/STAT3 signaling pathway is one of the most clearly described STAT3 phosphorylation pathways. In addition, Rho family proteins also play a significant role in regulating STAT3 phosphorylation and nuclear translocation [28, 29]. In gastrointestinal cancer cells, pPeOp interacts with GP130 by competing with IL-6 to activate the JAK family protease, thereby inhibiting the phosphorylation of STAT3 and playing an

antitumor role. In this process, the expression levels of JAK1, STAT3, and p-STAT3, the key factors of JAK/STAT3 signaling pathway, were significantly decreased, and the protein expression level of SOCS1, a negative feedback regulator of JAK/STAT3, was significantly up-regulated [8]. In addition, another regulator of STAT3 phosphorylation, the Rho family, is also inhibited by pPeOp, which can significantly inhibit the expression of Cdc42, Rac1, and the effector molecule, MgcRacGAP, thus cutting off the signal of promoting STAT3 phosphorylation from the abnormally expressed Rho family proteins in tumor cells [12].

In this study, we observed that HeLa cells showed significant shrinkage in morphology and decreased cell

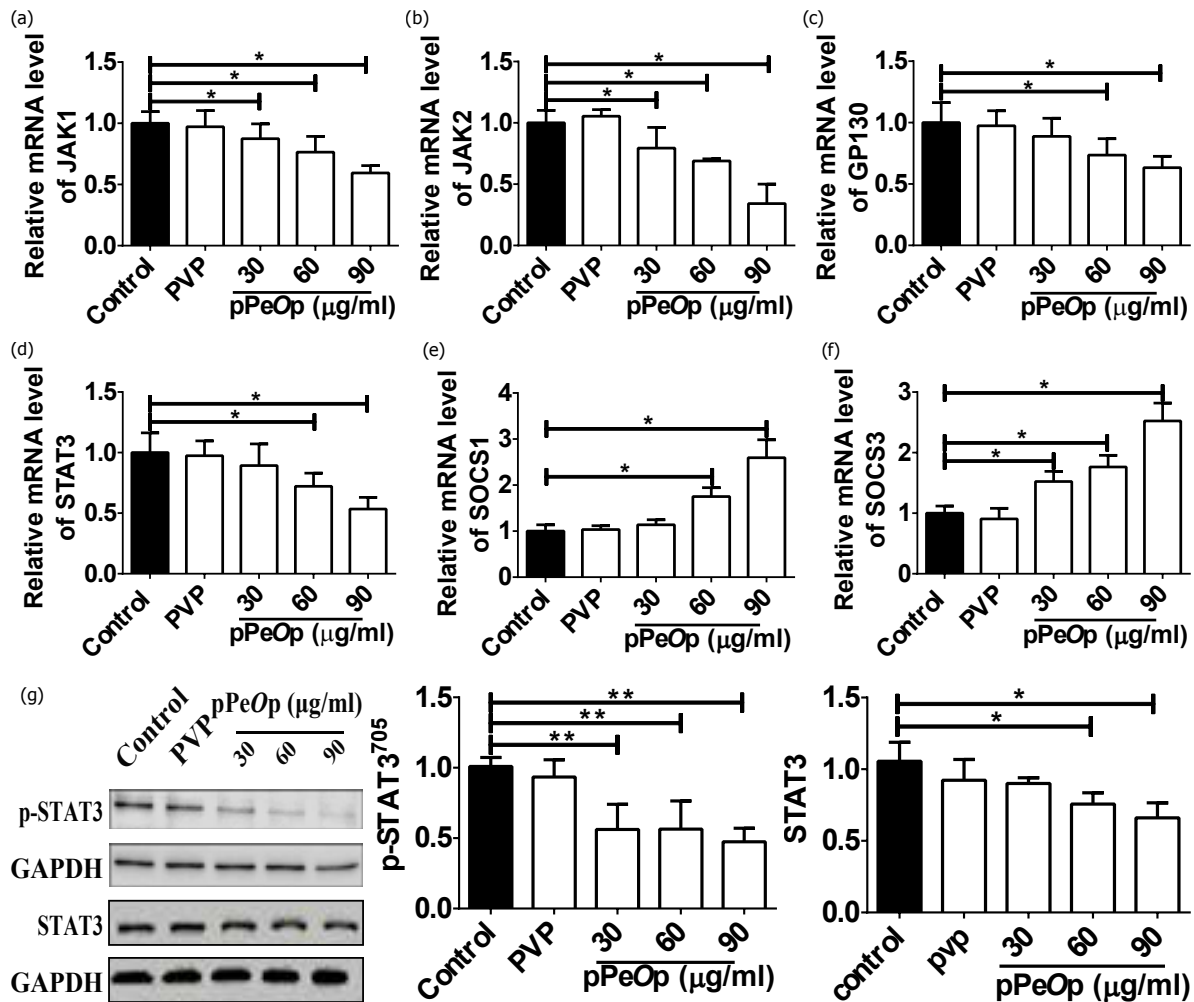


Fig. 2 Effects of pPeOp on JAK/STAT3 signaling pathway. HeLa cells were treated with PVP (90 µg/ml) or pPeOp (30, 60, and 90 µg/ml) for 24 h. (a–f) mRNA expression levels of JAK1, JAK2, GP130, STAT3, SOCS1, and SOCS3 detected by RT-qPCR. (g) Protein expression of STAT3 and p-STAT3 in HeLa cells detected by Western blot. Results are expressed as mean \pm SD from 3 separate experiments. * $p < 0.05$ and ** $p < 0.01$ vs. control group.

viability and proliferation ability after being treated with pPeOp for 24 h. RT-qPCR and Western blot results showed that after pPeOp treatment, the JAK/STAT3 signaling pathway in HeLa cells was significantly inhibited, and the expression levels of major genes in the pathway were significantly decreased such as JAK1, JAK2, GP130, and STAT3. In contrast, SOCS1 and SOCS3, which prevent STAT3 activation by competing with JAKs for STAT phosphorylation binding sites, were significantly elevated. The SOCS family consists of at least 8 members, namely SOCS1, SOCS2, SOCS3, SOCS4, SOCS5, SOCS6, SOCS7, and CIS (cytokine inducible SH2 containing protein) [18]. Members of the SOCS family are structurally similar, all of which contain n-terminal SH2 domain with varying lengths of amino acids and c-terminal conserved sequence composed of 40 amino acids, namely SOCS box [18].

SOCS is also a target gene of STAT, which is activated to promote transcription but in turn inhibits phosphorylation of STAT, thus forming a negative feedback regulatory chain [16, 18].

To further study the regulatory role of pPeOp on JAK/STAT3 signal pathway, IL-6 and NSC74859 were used in the present study as the agonist and inhibitor, respectively, of the JAK/STAT3 signaling pathway. IL-6 combining with GP130 activates the JAK/STAT3 signal pathway directly [30]. NSC74859 inhibiting STAT3 phosphorylation and blocking a homology dimer structure of STAT3 was widely used to study the JAK/STAT3 signaling pathway [31, 32]. RT-qPCR results suggested that IL-6 significantly activates JAK/STAT3 signal pathway, but the signal pathway was significantly inhibited when it acts with pPeOp together.

Through blocking proliferation and impairing via-

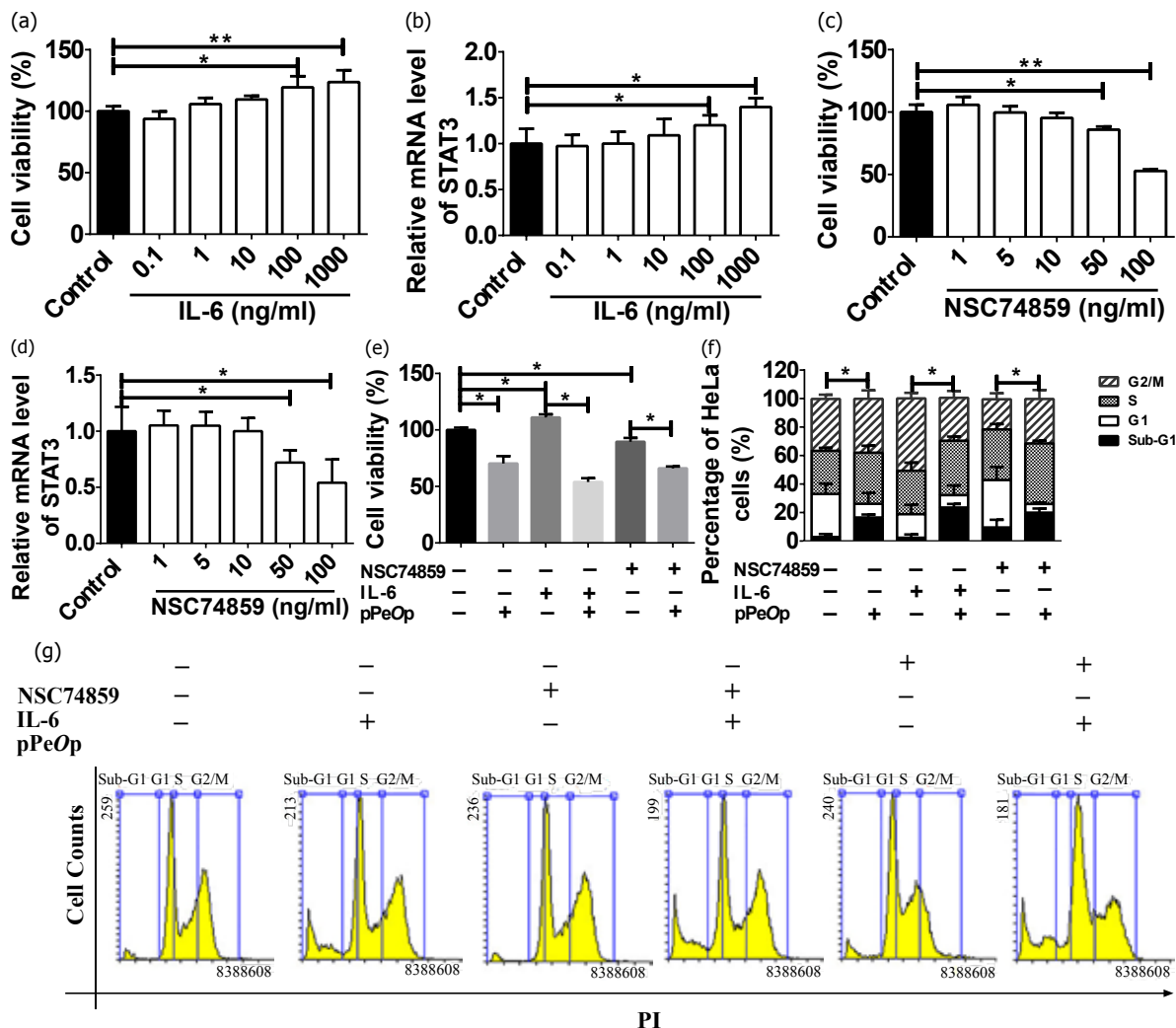


Fig. 3 Effects of pPeOp on HeLa cell cycle. (a–d) Selection of optimum concentration of agonists and inhibitors. Cell viability and STAT3 mRNA expression level after treated with different doses of IL-6 (0.1, 1, 10, 100, and 1000 ng/ml) or NSC74859 (1, 5, 10, 50, and 100 ng/ml) for 24 h. (e) Cell viability tested by MTS assay. (f–g) Cell cycle distribution analyzed by flow cytometry. HeLa cells were treated with pPeOp (60 μg/ml) for 24 h in the absence or presence of NSC74859 (50 ng/ml) or IL-6 (100 ng/ml). * $p < 0.05$ and ** $p < 0.01$ vs. control group.

bility of cervical cancer cells, the antitumor effects of pPeOp have been proved. It is worth noting that the antitumor effects of pPeOp increased when pPeOp was co-treated with IL-6, whereas NSC74859 weakened the antitumor effect of pPeOp. PI, a classic fluorescent dye, combines with DNA to emit strong red fluorescence [33]. Detecting the fluorescence intensity of PI binding by flow cytometry, the amount of DNA in the cell is accurately reflected. According to the amount of DNA, the cell cycle is divided into Sub-G1 phase, G1 phase, S phase, and G2 phase [34]. It is reported that cell death is related to DNA damage and degradation [35]. Hence, cells in Sub-G1 phase were regarded as dead cells. In the present study,

the proportion of Sub-G1 in cervical cancer cells was significantly increased after treating with pPeOp. IL-6 significantly increased cells in sub-G1 phase after treating with pPeOp, which was consistency with MTS results. Therefore, the *in vitro* data demonstrated that pPeOp could effectively inhibit the proliferation and viability of cervical cancer cells possibly by regulating JAK/STAT3 signaling pathway.

In conclusion, in terms of cell characterization, pPeOp could significantly shrink the surface of HeLa cells and significantly reduce cell activity and proliferation ability. From the perspective of molecular regulation mechanism, pPeOp has a significant negative regulation effect on JAK/STAT3 signaling pathway in

HeLa cells and thus inhibits cell cycle. Traditional Chinese medicine has multi-component and multi-target efficacy and is less likely to produce drug resistance and other characteristics. Therefore, pPeOp is a very promising candidate for cervical cancer treatment.

Acknowledgements: This project was supported by the National Natural Science Foundation of China (Grant No. 81874355 and Grant No. 82174028).

REFERENCES

- Vu M, Yu J, Awolude OA, Chuang L (2018) Cervical cancer worldwide. *Curr Probl Cancer* **42**, 457–465.
- Arbyn M, Weiderpass E, Bruni L, de Sanjosé S, Saraiya M, Ferlay J, Bray F (2020) Estimates of incidence and mortality of cervical cancer in 2018: a worldwide analysis. *Lancet Glob Health* **8**, e191–e203.
- Gauri A, Messiah SE, Bouzoubaa LA, Moore KJ, Koru-Sengul T (2020) Cervical cancer sociodemographic and diagnostic disparities in Florida: a population-based study (1981–2013) by stage at presentation. *Ethn Health* **25**, 995–1003.
- Jr WS, Bacon MA, Bajaj A, Chuang LT, Fisher BJ, Harkenrider MM, Jhingran A, Kitchener HC, et al (2017) Cervical cancer: A global health crisis. *Cancer* **123**, 2404–2412.
- Ohno N, Miura T, Saito K, Nishijima M, Miyazaki T, Yadomae T (1992) Physicochemical characteristics and antitumor activities of a highly branched fungal (1- β -D-glucan, OL-2, isolated from *Omphalia lapidescens*. *Chem Pharm Bull (Tokyo)* **40**, 2215–2218.
- Saito K, Nishijima M, Ohno N, Yadomae T, Miyazaki T (1992) Structure and antitumor activity of the less-branched derivatives of an alkali-soluble glucan isolated from *Omphalia lapidescens*. (Studies on fungal polysaccharide. XXXVIII). *Chem Pharm Bull (Tokyo)* **40**, 261–263.
- Zhang G, Huang Y, Bian Y, Wong JH, Ng TB, Wang H (2006) Hypoglycemic activity of the fungi *Cordyceps militaris*, *Cordyceps sinensis*, *Tricholoma mongolicum*, and *Omphalia lapidescens* in streptozotocin-induced diabetic rats. *Appl Microbiol Biotechnol* **72**, 1152–1156.
- Chen L, Lu Z, Yang Y, Du L, Zhou X, Chen Y (2018) Effects of purified *Omphalia lapidescens* protein on metastasis, cell cycle, apoptosis and the JAK-STAT signaling pathway in SGC-7901 human gastric cells. *Oncol Lett* **15**, 4161–4170.
- Chen YT, Lu QY, Lin MA, Cheng DQ, Ding ZS, Shan LT (2011) A PVP-extract fungal protein of *Omphalia lapideacens* and its antitumor activity on human gastric tumors and normal cells. *Oncol Rep* **26**, 1519–1526.
- Yang YL, Gong WY, Chen FF, Chen LC, Chen YT (2017) pPeOp from *Omphalia lapidescens* Schroet induces cell cycle arrest and inhibits the migration of MC-4 gastric tumor cells. *Oncol Lett* **14**, 533–540.
- Lu Z, Xu W, Lin M, Zhou X, Chen Y (2018) Growth inhibition and apoptosis induction of pPeOp protein in human colon cancer cell line SW620. *Int J Clin Exp Med* **11**, 5683–5690.
- Xu Y, Xu W, Lu Z, Cheung MH, Lin M, Liang C, Lou J, Chen Y (2021) Anti-gastric cancer effect of purified *Omphalia lapidescens* protein via regulating the JAK/STAT3 signaling pathway. *Nutr Cancer* **74**, 1780–1791.
- Yu H, Jove R (2004) The STATs of cancer-new molecular targets come of age. *Nat Rev Cancer* **4**, 97–105.
- Marquina G, Manzano A, Casado A (2018) Targeted agents in cervical cancer: Beyond bevacizumab. *Curr Oncol Rep* **20**, 40.
- Wolford JE, Tewari KS (2018) Rational design for cervical cancer therapeutics: cellular and non-cellular based strategies on the horizon for recurrent, metastatic or refractory cervical cancer. *Expert Opin Drug Discov* **13**, 445–457.
- Villarino AV, Kanno Y, O'Shea JJ (2017) Mechanisms and consequences of Jak-STAT signaling in the immune system. *Nat Immunol* **18**, 374–384.
- Bharadwaj U, Kasembeli MM, Robinson P, Twardy DJ (2020) Targeting Janus kinases and signal transducer and activator of transcription 3 to treat inflammation, fibrosis, and cancer: Rationale, progress, and caution. *Pharmacol Rev* **72**, 486–526.
- Shuai K, Liu B (2003) Regulation of JAK-STAT signalling in the immune system. *Nat Rev Immunol* **3**, 900–911.
- Darnell Jr JE (1997) STATs and gene regulation. *Science* **277**, 1630–1635.
- Lim CP, Cao X (2006) Structure, function, and regulation of STAT proteins. *Mol Biosyst* **2**, 536–550.
- Abroun S, Saki N, Ahmadvand M, Asghari F, Salari F, Rahim F (2015) STATs: An old story, yet mesmerizing. *Cell J* **17**, 395–411.
- Banerjee K, Resat H (2016) Constitutive activation of STAT3 in breast cancer cells: A review. *Int J Cancer* **138**, 2570–2578.
- Chuang CH, Greenside PG, Rogers ZN, Brady JJ, Yang D, Ma RK, Caswell DR, Chiou SH, et al (2017) Molecular definition of a metastatic lung cancer state reveals a targetable CD109-Janus kinase-Stat axis. *Nat Med* **23**, 291–300.
- Swamy SG, Kameshwar VH, Shubha PB, Looi CY, Shanmugam MK, Arfuso F, Dharmarajan A, Sethi G, et al (2017) Targeting multiple oncogenic pathways for the treatment of hepatocellular carcinoma. *Target Oncol* **12**, 1–10.
- Browning L, Patel MR, Horvath EB, Tawara K, Jorcyk CL (2018) IL-6 and ovarian cancer: inflammatory cytokines in promotion of metastasis. *Cancer Manag Res* **10**, 6685–6693.
- Zhang F, Wang Z, Fan Y, Xu Q, Ji W, Tian R, Niu R (2015) Elevated STAT3 signaling-mediated upregulation of MMP-2/9 confers enhanced invasion ability in multidrug-resistant breast cancer cells. *Int J Mol Sci* **16**, 24772–24790.
- Zou M, Zhang X, Xu C (2016) IL6-induced metastasis modulators p-STAT3, MMP-2 and MMP-9 are targets of 3,3'-diindolylmethane in ovarian cancer cells. *Cell Oncol (Dordr)* **39**, 47–57.
- Zhao C, Qi L, Chen M, Liu L, Yan W, Tong S, Zu X (2015) microRNA-195 inhibits cell proliferation in bladder cancer via inhibition of cell division control protein 42 homolog/signal transducer and activator of transcription-3 signaling. *Exp Ther Med* **10**, 1103–1108.
- Geletu M, Guy S, Arulanandam R, Feracci H, Raptis L (2013) Engaged for survival: from cadherin ligation to stat3 activation. *JAK-STAT* **2**, e27363.

30. Kang S, Tanaka T, Narazaki M, Kishimoto T (2019) Targeting interleukin-6 signaling in clinic. *Immunity* **50**, 1007–1023.
31. Wang Z, Li J, Xiao W, Long J, Zhang H (2018) The STAT3 inhibitor S3I-201 suppresses fibrogenesis and angiogenesis in liver fibrosis. *Lab Invest* **98**, 1600–1613.
32. Nishimura K, Goto K, Nakagawa H (2018) Effect of erythropoietin production induced by hypoxia on autophagy in HepG2 cells. *Biochem Biophys Res Commun* **495**, 1317–1321.
33. Bode KJ, Mueller S, Schweinlin M, Metzger M, Brunner T (2019) A fast and simple fluorometric method to detect cell death in 3D intestinal organoids. *Biotechniques* **67**, 23–28.
34. Meng Q, Tang B, Qiu B (2019) Growth inhibition of Saos-2 osteosarcoma cells by lactucopicrin is mediated via inhibition of cell migration and invasion, sub-G1 cell cycle disruption, apoptosis induction and Raf signalling pathway. *J BUON* **24**, 2136–2140.
35. Chang YM, Shih YL, Chen CP, Liu KL, Lee MH, Lee MZ, Hou HT, Huang HC, et al (2019) Ouabain induces apoptotic cell death in human prostate DU 145 cancer cells through DNA damage and TRAIL pathways. *Environ Toxicol* **34**, 1329–1339.